International Journal of Engineering and Advanced Technology (IJEAT)
ISSN: 2249-8958 (Online), Volume-8 Issue-5, June 2019

Digital Processing of Location Monitoring Reflectograms of Overhead Transmission Lines

V.A. Kasimov

Abstract: ***This article discusses methods of digital signal processing. Processing procedure of reflectograms of location testing in the case of ice coatings on power lines is developed. Due to abnormal dispersion in ice, the reflected location signals, upon existence on ice coatings, are dispersed in time, however, the shape of reflected signal is retained upon extraction of reflected location signals in narrow frequency band. Possible methods of suppression of narrow band interferences are described as well as methods of time–frequency analysis of reflectograms.***

Index Terms: ***overhead transmission line (OTL), location testing, ice coatings on power lines, digital signal processing, time–frequency analysis.***

I. INTRODUCTION

Ice coating on wires of overhead transmission lines (OTL) can lead to serious emergency situations. In order to prevent such situations, it is necessary to monitor continuously the state of power lines. According to monitoring results, upon occurrence of ice coating which could cause emergency situations, such coatings are melted. Kazan State Power Engineering University starting from 1995 carries out research devoted to detection of ice coatings on power lines by location method, as well as damages of OTL [1-4]. At present more than 1,000,000 reflectograms of 35–330 kV OTL were recorded using six location complexes which monitor the state of OTL in Russia. Such studies are unique and have no analogues in the world. Therefore, it was required to develop efficient processing procedure for reflectograms of location monitoring of OTL. Upon location diagnostics of OTL, the information about its state is contained in reflectogram: response to testing signal. Damages or ice coatings result in certain distortions of reflectograms. Hence, it is very important to process reflectograms in order to obtain information about these distortions which can be applied for determination of damage type and sizes of ice coatings. Under conditions of ice coating generation on OTL, the variations of attenuation and delay (speed) of reflected location signals strongly depend on their frequency in operation frequency band (16–1,000 kHz) [5]. Since the location video pulse is wideband, such variations during increase in the wall thickness of ice coatings lead to variations in form and distribution of power of spectral components of reflected pulse. In this case the wall thickness of ice coatings on wires can be determined by narrowband components of wideband reflected location signal. Reflectogram processing both upon monitoring of ice coatings and upon detection of damages is characterized by the fact that location facility operates generally in parallel with equipment of engineering communication via transmission lines [6]. Signals of these instruments interfere with the signals of location testing. It is known that under conditions of ice coating generation on OTL, the variations of attenuation and delay (speed) of reflected location signals strongly depend on their frequency. Since in our case the reflected pulse is wideband, such variations during increase in the wall thickness of ice coatings lead to variations in form of signals as well as frequency distribution of power of reflected location pulse. In this case the displacements of wideband signals determined using cross correlation are characterized by statistic similarity of signals but due to distortions of form and spectrum of reflected pulse, cannot be used for detection of wall thickness of ice coatings on wires. In order to determine correctness of predictions of wall thickness of ice coatings, it was proposed to extract components of wideband reflected location signal in narrow frequency band and to determine their attenuation and delay.

Manuscript published on 30 June 2019.
***** Correspondence Author (s)
V.A. Kasimov*, Kazan State Power Engineering University, Kazan, Russia.

II. METHODS

In this regard the most urgent issue is development of numerical processing of reflectograms of OTL carrier links. In its turn this requires for: 1) detection of interferences; 2) suppression of interferences; 3) analysis of reflected location signals for selection of extraction band of their components; 4) extraction of narrowband components of wideband reflected location signals [7].

Detection of narrowband interferences

Signal constraint in time is equivalent to the product of finite rectangular window and infinite signal; according to the convolution theorem, the obtained spectrum is the convolution of infinite signal spectrum and spectrum of rectangular window. The spectrum of rectangular window is described by sinc function with the side lobe level of –13 dB which causes dispersion of signals spectra upon convolution. This dispersion is the most obvious for power narrowband signals presented by interferences in this case.

In order to decrease this effect, the weight method is widely used or smoothing by windows. Upon smoothing, frequency resolution of closely positioned narrowband signals can be deteriorated due to increase in width of main lobe of window function spectrum, however, resolution of multilevel (in terms of power) narrowband signals (not closely positioned) is generally improved.

Spectrum smoothing of reflectograms of K. Bukash–R. Sloboda OTL using Blackman–Harris window is exemplified in Fig. 1 which illustrates decrease in dispersion of interference spectra of HF appliances in the frequency band near 200, 540, 800, and 900 kHz due to spectrum smoothing. The smoothing made it possible to detect signals of lower power at 100, 500, 600, 750, and 880 kHz (Fig. 1), however, the smoothed spectrum was highly peaked.

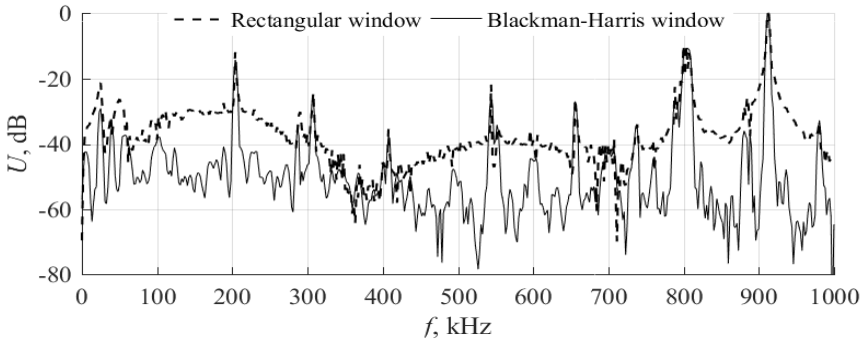

Fig. 1: Normalized spectra of reflectogram of K. Bukash–R. Sloboda OTL with smoothing by Blackman–Harris window and rectangular window (equivalent to spectrum without smoothing).

Less peaked frequency characteristic can be obtained by the MUSIC (MUltiple SIgnal Classification) or EV (EigenVectors) methods. These methods are intended for detection of frequency and estimation of level of sinusoid signals and not for detection of spectrum itself, thus, the obtained frequency dependences are referred to as pseudospectra. Figure 2 illustrates normalized smoothed spectrum of reflectograms and pseudospectra obtained by the EV and MUSIC methods (their plots nearly coincide). These methods give similar results and provide detection of close multilevel (in terms of power) narrowband interfering signals comparable with smoothed spectrum and overriding classical Fourier spectrum (Fig. 1).

After determination of frequency position and evaluation of levels of harmonic interferences, it is necessary to suppress the detected interferences.

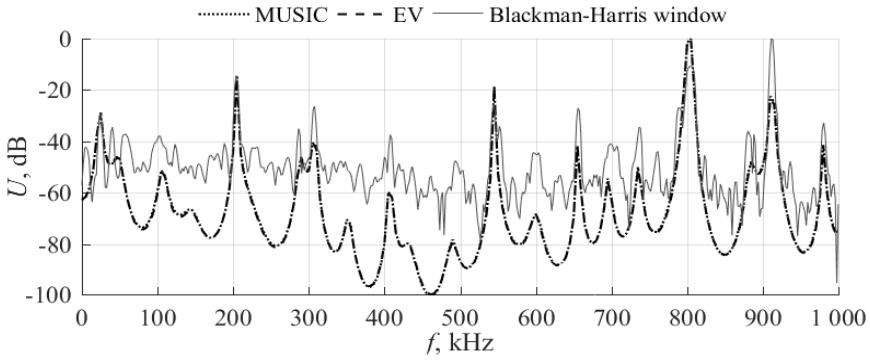

Fig. 2: Normalized spectra with smoothing by Blackman–Harris window and pseudospectra obtained by EV and MUSIC methods, reflectograms of K. Bukash–R. Sloboda OTL.

Suppression of narrowband interferences

Interferences are also suppressed by weight functions. Using these functions, the impulse response of filter is smoothed. Side effect is the increase in the width of filter transition band, however, for the considered problem of interference suppression, the main issue is provision of sufficient filter attention in rejection region.

Synthesis of filters using windows is carried out using inverse Fourier transform of preset filter AFC, then the obtained impulse response is symmetrically truncated by window function to the size equaling to the order of filter $N + 1$. Signals are filtrated using linear convolution of filter impulse response with signal counting.

Window smoothing of impulse response decreases the level of side lobes of AFC filter, decreases inhomogeneity in free transmission band and increases attenuation in the rejection region, however, leads to widening filter transmission band.

Thus, synthesized filters are referred to the class of linear filters with finite impulse response (FIR), otherwise, nonrecursive, that is, without feedbacks between filter output and input.

In addition, filtration can be carried out using recursive filters with infinite impulse response (IIR), such as Butterworth filters, Chebyshev filters of the first and second kind, and elliptic filters (Cauer or Cauer–Zolotarev filters). Herewith, the required filter AFC is approximated by nominal functions. The variables upon computations of IIR of filters can be pulsation levels in free transmission band and in rejection band as well as initial and final frequencies of transmission bands.

Generally, the elliptic filters, other requirements to the considered filter being equal, are characterized by the lowest order and, as a consequence, the least computational difficulty for signal filtration, including that compared with FIR filters.

One of peculiarities of IIR filters is nonlinearity of phase frequency characteristic (PFC) which can lead to distortion of reflected location impulse. PFC can be linearized by double passing signal via filter inverting the signal in time before and after repeated filtration, thus, upon the repeated filtration the PFC, nonlinearity is compensated resulting in group zero delay.

However, development of multiband IIR filters providing suppression of all narrowband interferences is more complicated task in comparison with development of window FIR filters; such IIR filter will be comprised of cascade of rejection filters, each of them should be developed separately. Since the procedure of interference suppression is not time determining stage of numerical processing of reflectograms of OTL location testing, filtration is performed using FIR filters, since they are simpler synthesized in comparison with IIR filters.

Figure 3 illustrates the results of interference suppression on the reflectogram of K. Bukash–R. Sloboda OTL measured without signal accumulation. It should be mentioned that upon location testing, the distance to the point of reflection is determined by the time and propagation speed of signal. Thus, for convenience of reflectogram analysis, the distance scale is used instead of time scale. The propagation speed of signals can vary, however, aiming at plot construction, the speed is assumed to be equal to the speed of light. Then, with account for double passing of signals before and after reflection, the propagation time $\tau = 1\ \mu s$ is associated with the distance $L = (1\ \mu s) \times (3 \cdot 10^8\ m/s)/2 = 150\ m$.

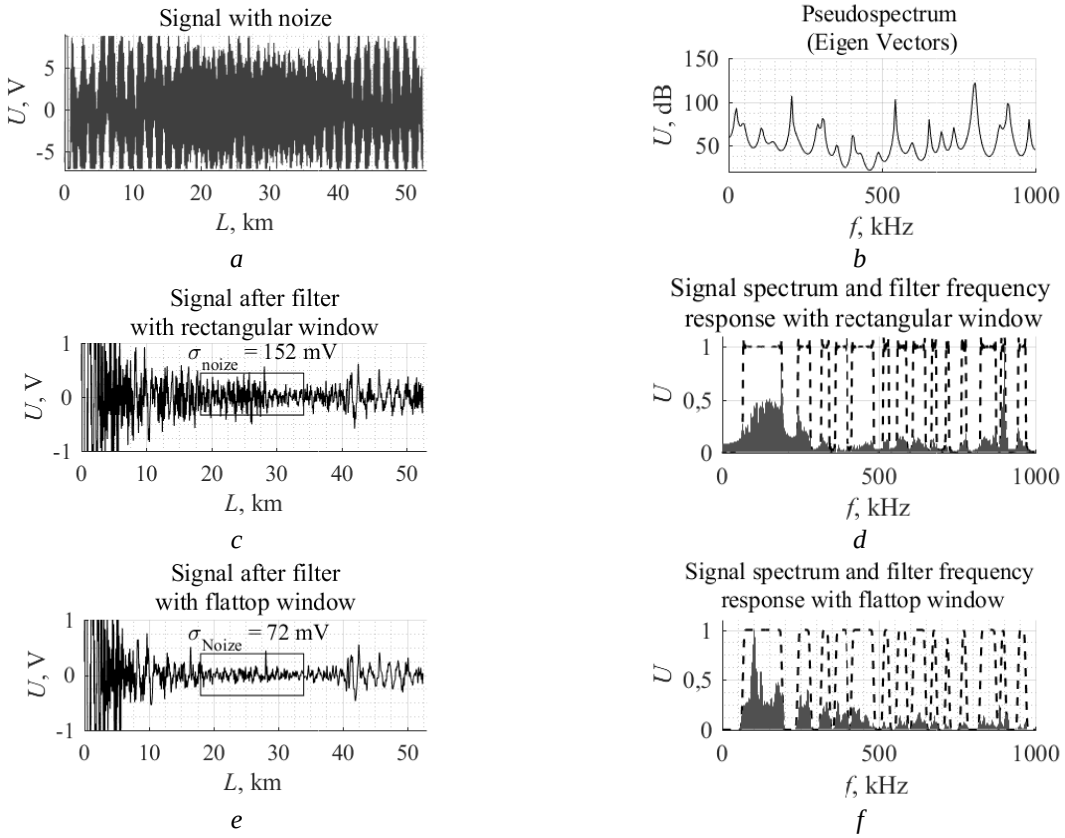

Fig. 3: Reflectogram of K. Bukash–R. Sloboda OTL before (*a*) and after (*c*, *e*) and respective pseudospectrum (*b*), normalized spectra and AFC filters (*d*, *f*), smoothed by rectangular window (*c*, *d*) and flattop window (*e*, *f*).

Figure 3, *a* illustrates initial reflectogram filled with modulated harmonic interfering signals from HF appliances with the amplitude of about 6–7 V. Figure 3, *b* illustrates pseudospectrum of this reflectogram (Fig 3, *a*) used for determination of frequency of harmonic interferences. The pseudospectrum, in addition to interferences from the appliances supporting this line and operating in the frequency range from 750 to 950 kHz, demonstrates reliably interferences induced from other OTL.

Figures 3, *c* and *e* illustrate signals after FIR filtration with smoothing by rectangular window (*c*) which is equivalent to filter without smoothing and flattop window (*e*). It can be seen in this plots that the filter with smoothing by flattop window (Fig. 3, *e*) provides better suppression of interferences: mean square deviations of noises (in time region without reflected signal highlighted by rectangle) vary by about two times (152 mV for rectangular window and 72 mV for flattop window).

Figures 3, *d* and *f* reflect normalized spectra of filtered signals and AFC filters with smoothing by rectangular window and flattop window, respectively.

Published By:
Blue Eyes Intelligence Engineering
& Sciences Publication (BEIESP)

Figure 3, *d* illustrates AFC pulsations in the free transmission band, it is possible to observe dispersion of spectrum and incomplete suppression of signals in attenuation region mentioned above. Using window smoothing (Fig. 3, *f*), these effects are nearly completely eliminated or, at least, significantly reduced. This example is based on flattop window because it provides the lowest pulsations in the free transmission band. The use of FIR filters with high attenuation of side lobes in rejection band and, as a rule, high pulsations does not lead to decrease in the noise level, and the flattop window is characterized by the lowest noise level, that is, the best suppression of interferences.

Analysis of reflected location signals

After suppression of interferences, it is necessary to analyze reflected location signal in order to select frequency and time range of its processing, that is, it is necessary to determine time–frequency distribution of power of reflected location signal. Two approaches were proposed: separate determination of time and frequency distribution and combined determination of time–frequency distribution of signal power.

Time–frequency power distribution of location signals

In order to determine time distribution of power, the algorithms of prediction of amplitude envelope of $A(t)$ signal were developed. In the case of complement of $s(t)$ signal with its quadrature complement $s_1(t)$ (imaginary copy with phase shift π/2), the analytical signal is obtained: $\dot{s}_a(t) = s(t) + js_1(t)$. Absolute magnitude of such analytical signal is the amplitude envelope of complex signal $A(t) = |\dot{s}_a(t)| = \sqrt{s^2(t) + s_\perp^2(t)}$.

Quadrature complement is determined by the Gilbert transform: $s_\perp(t) = \frac{1}{\pi}\int_{-\infty}^{\infty} \frac{s(t')}{t-t'} dt'$. AFC of the transform equals to unity at all frequencies except for zero where it equals to zero, and PFC in the region of positive frequencies shifts the phase by $-\pi/2$, and in the region of negative frequencies – by $\pi/2$. Due to such transform, the spectrum of analytical signal in the region of negative frequencies is zero, remains the same at zero frequency, and is doubled in the region of positive frequencies.

Figure 4 illustrates the plots of initial signal, its quadrature complement, and amplitude envelope of signal in time region of reflected signal. Using the plot of amplitude envelope, the time interval is determined where the main power of reflected location signal is concentrated. This range for the given example (Fig. 4) is in the limits of from 40 to 43 km. This example is sufficiently trivial, however, for the extracted in narrow frequency band and/or more noise contaminated signals, the plot of amplitude envelope could be useful.

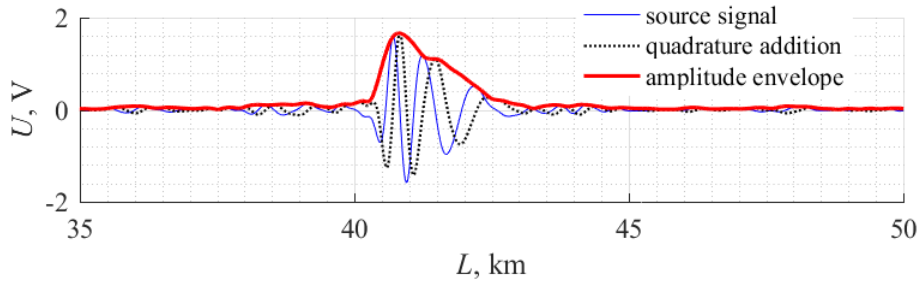

Fig. 4: Reflected location signal, its quadrature complement and amplitude signal envelope of K. Bukash–R. Sloboda OTL.

Frequency distribution of power of reflected location signal can be determined by the spectrum of reflected signal in the time range containing this signal. Figure 5 illustrates the spectra of reflected location signal (for time regions of 40–43 km and 37–46 km) and theoretical spectrum for testing rectangular impulse with the duration of 2 μs.

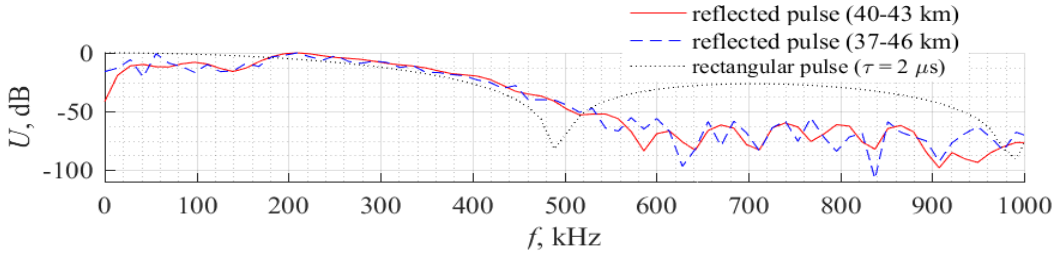

Fig. 5: Normalized spectra of reflected location signal (time bands: 40–43 and 37–46 km, solid and dashed curves, respectively) and spectrum of rectangular pulse (duration: $\tau = 2$ μm, dotted curve).

The shape of impulse spectrum somewhat depends on the range selection (Fig. 5). High frequency components in carrier links attenuate stronger, which stipulates divergence of spectra of theoretical rectangular and reflected impulse. Divergences in the frequency bands up to 50 kHz are also stipulated by carrier link AFC.

While determining spectrum of reflected impulse, the impact of window functions on signal in time region should be taken into account: upon window smoothing, the counts at start and end of signal are suppressed, which is not critical for harmonic signals, however, upon determination of spectrum of reflected location impulse, their components at the start and end of impulse are suppressed. Thus, despite the mentioned drawbacks, the frequency distribution of power of reflected location impulse should be determined using common Fourier transform.Amplitude envelope and spectrum of reflected location signal determine the time and the frequency distributions, respectively. Combined time and frequency distribution is determined by means of time–frequency

transforms.

Time–frequency power distribution of location signals

Distribution based on the Fourier transform is the simplest. Herewith, reflectogram is subdivided into segments, for each segment the spectrum is determined using weight functions. Combination of these spectra forms spectrogram. A disadvantage of this approach is inverse dependence of resolutions in terms of frequency and time ($t \cdot \Delta f \geq 1$). In terms of uncertainties, the best time–frequency localization is characteristic for transform with Gauss window, also known as the Gabor transform. Moreover, this uncertainty can be decreased by subdivision into overlaying segments.

Time–frequency distribution of power in addition to linear Fourier transform and its modifications are analyzed by widely applied nonlinear transforms of the Cohen class based on the Wigner (Wigner–Will) transform [8], [9]:

$$P_V(\omega,t)=\int_{-\infty}^{\infty}\dot{s}_a\left(t+\frac{\tau}{2}\right)\dot{s}_a^*\left(t-\frac{\tau}{2}\right)e^{-i\omega\tau}d\tau, \quad (1)$$

where $\dot{s}_a$ is the analytical signal determined by Gilbert transform, $\dot{s}_a^*$ is its complex conjugate signal.

It provides good time–frequency resolution, however, there are peculiarities which are absent in the Fourier transform. The obtained result can be negative in some regions, that is, it is not complete function of spectral density. The transform nonlinearity determines the second peculiarity: existence of interference (cross) effects for multicomponent signals.

At present the methods are available which can decrease interference, however, time–frequency resolution can be deteriorated.

For frequency smoothing the $h(\tau)$ window in time region is used:

$$P_{PV}(\omega,t)=\int_{-\infty}^{\infty}\boldsymbol{h(\tau)}\dot{s}_a\left(t+\frac{\tau}{2}\right)\dot{s}_a^*\left(t-\frac{\tau}{2}\right)e^{-i\omega\tau}d\tau. \quad (2)$$

Due to such smoothing, the frequency resolution is somewhat deteriorated, such modification is referred to as Wigner pseudo-transform.

Further modification assumes to apply the window $h(\tau)$ together with the smoothing window $g(u)$. This smoothed Wigner pseudo-transform is written as follows:

Other modifications also exist, such as the Choi–Williams and Born–Jordan transforms which suppress interference nonsymmetrically: mainly along the lines $\omega = const$ and $t = const$, respectively, or RID (Reduced Interference

$$P_{SPV}(\omega,t)=\int_{-\infty}^{\infty}h(\tau)\int_{-\infty}^{\infty}\left(\boldsymbol{g(u-t)}\dot{s}_a\left(u+\frac{\tau}{2}\right)\dot{s}_a^*\left(u-\frac{\tau}{2}\right)du\right)e^{-i\omega\tau}d\tau \quad (3)$$

Distribution) in the following form [10]:

Figure 6 illustrates spectrogram of reflectograms of K. Bukash–R. Sloboda OTL with interferences obtained by RID, and its analysis.

Nonlinear transform is characterized by significantly better resolution both in terms of time and frequency, which

$$P_{RID}(\omega,t)=\int_{-\infty}^{\infty}h(\tau)\int_{-\frac{|\tau|}{2}}^{\frac{|\tau|}{2}}\left(\frac{g(u)}{|\tau|}\left(1+\cos\frac{2\pi u}{\tau}\right)\dot{s}_a\left(t+u+\frac{\tau}{2}\right)\dot{s}_a^*\left(t+u-\frac{\tau}{2}\right)du\right)e^{-i\omega\tau}d\tau \quad (4)$$

provides detection of power signals. However, despite the modification, it is impossible to eliminate completely interference terms which are observed, for instance, in the time region from 10 to 35 km (Fig. 6), and it prevents detection of reflections from heterogeneities of wave resistance of OTL carrier links caused by wire grounding at the distances of about 12, 18, 25, and 30 km. In addition, suppression of interferences initiates certain interference disturbance, for instance, as a consequence of interference suppression at 200 kHz (Fig. 6, *b*), interferences occur near this frequency at the entry and end of signal.

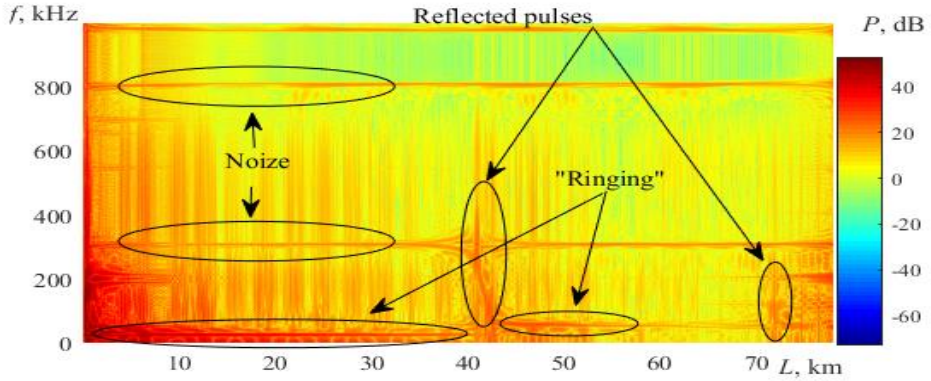

Fig. 6: Spectrogram of RID reflectograms of K. Bukash–R. Sloboda OTL and its interpretation.

Published By:
Blue Eyes Intelligence Engineering
& Sciences Publication (BEIESP)

In addition to the above considered methods, the signals were analyzed by the wavelet method and empirical mode decomposition (Gilbert–Huang transform) [11]. However, due to limited scope of the work and unrevealed significant advantages with regard to the described methods, these methods are not described in this work. A promising approach to description and analysis of reflectograms of location testing is the use of Prony series [12].

Distribution of power should be analyzed using the Wigner distribution with decreased interference, which is characterized by the best time–frequency resolution of all considered distributions. In order to detect and to exclude interference terms from consideration, it is required to apply either amplitude envelope and spectrum of reflected signal, or smoothed Fourier spectrogram with overlaid segments.

Extraction of narrowband constituents of reflected location signals

Upon extraction of useful reflected location signal, the requirements to filter somewhat vary. Pulsations in the filter free passing band and sharp narrowing of signal spectrum by narrow transient bands cause dispersion of signal in time region, thus, in order to extract signals in narrow band near central (working) frequency, in addition to the aforementioned filters a resonator of the second order was used (peak filter, analog of single oscillating circuit) which was an IIR filter.

Variables of this filter are central frequency, width of free transmission band, and the level for determination of free transmission band: –3 dB by default. Since this filter has nonlinear PFC, two cascades are used for compensation of nonlinearity, each with one half attenuation. This filter has smooth AFC, which stipulates lower attenuation in rejection band in comparison with the filters considered above.

Figure 7 illustrates extractions of reflected signal in the frequency band of 120–140 kHz using various filters. Due to smoother variation of attenuation of filter –resonator, the lowest dispersion of reflected location signal in time region is provided (Fig. 7).

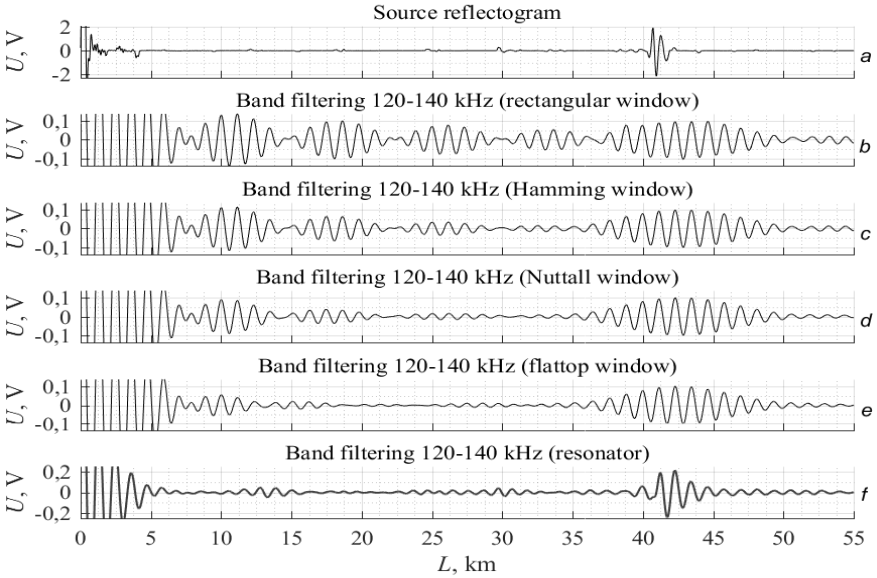

Fig. 7: Extraction of components of reflected location signal in frequency band of 120–140 kHz with various filters in reflectogram of K. Bukash–R. Sloboda OTL.

Figure 8 illustrates the components of reflected location signals extracted in the band of 120–140 kHz with and without ice coatings on K. Bukash – R. Sloboda OTL as well as reflected signal in wide band (75–500 kHz). The extraction was carried out by two filters: resonator of the second order and filter with smoothed (flattop window) impulse characteristic. Aiming at comparison with regular signal (without ice coating), in Fig. 8 the reflected signal with ice coatings (bold line) was shifted by 3.78 μs and amplified twice (dotted line) which made it possible to compensate partially the influence of ice coatings on propagation of signals.

It was demonstrated (Fig. 8) that upon extraction of reflected signal in narrow frequency band, its shape was nearly not distorted under the influence of ice coatings, and due to amplification and shift of signal, the influence of ice coating on reflected signal could be compensated which was observed both for the resonator of the second order and for the filter based on flattop window, i.e. the attenuation provided by resonator was sufficient for extraction in narrow band and near central operating frequency.

Published By:
Blue Eyes Intelligence Engineering
& Sciences Publication (BEIESP)

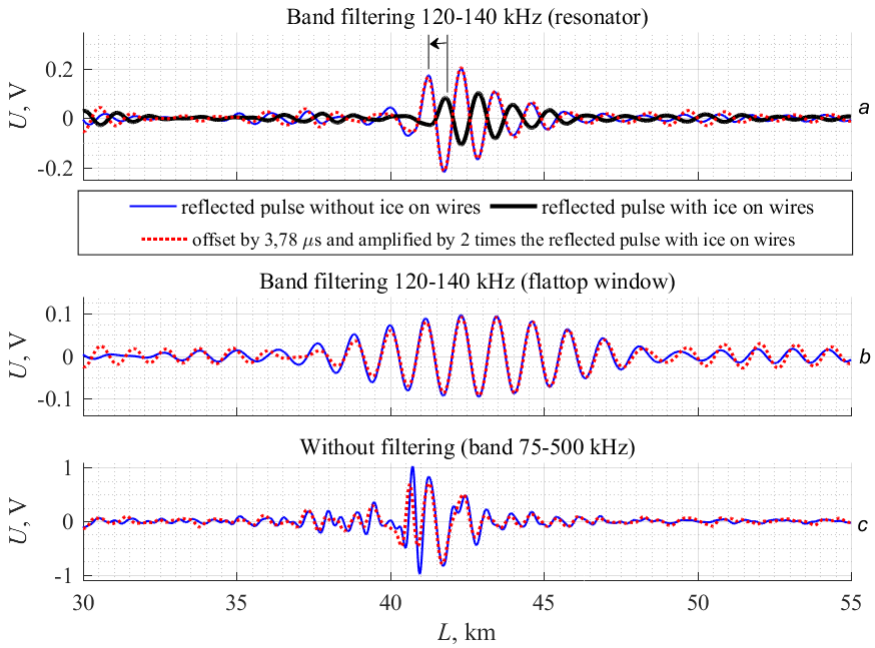

Fig. 8: Reflected location signals with and without ice coatings on wires of K. Bukash–R. Sloboda OTL.

Figure 8, *c* illustrates the wideband reflected signals; it can be seen that due to similar cases (Fig. 8, *a*, *b*) of signal amplification and displacement, the influence of ice coating could not be compensated. If at the end of reflected impulse (41.5–44 km) the signals nearly coincide, then at initiation of impulse (40–41.5 km) excessive displacement and insufficient amplification are observed, that is, the initial segment of reflected impulse is characterized by higher attenuation and lower delay. This is stipulated by the fact that high frequency signals have higher propagation speed in OTL carrier link, hence, high frequency components of signal are concentrated at beginning of reflected impulse. It is known that upon ice coating generation, additional attenuation increases with frequency and additional delay decreases, which stipulates lower delay and higher attenuation of initial segment of reflected impulse in comparison with final segment where lower frequency components are concentrated.

III. CONCLUSION

Therefore, the procedure is proposed for digital processing of reflectograms of OTL for predictions of attenuation and delay of location signals under conditions of ice coating generation on OTL, which considers for decrease in propagation speed of electromagnetic waves accompanied by their additional attenuation, these variations are characterized by frequency dependence. This procedure is comprised of four main stages:

1) detection of harmonic interferences of HF appliances by reflectogram spectrum; window smoothing of spectra decreases their dispersing which leads to overlaying of some interferences with dispersed spectra of more power interfering signals;

2) suppression of detected harmonic interferences by nonrecursive filters provides sufficient attenuation in rejection band of synthesized filters;

3) analysis and selection of extraction range of narrowband components of wideband reflected location signals using system approach based on Gilbert, Fourier, and Wigner time–frequency transforms;

4) extraction of narrowband components of wideband reflected location signals by digital recursive analog of oscillating circuit (two cascades for compensation of nonlinearity of its PFC) characterized by continuous AFC and providing the lowest dispersing in time of narrowband components of wideband reflected location signals;

Then attenuation and delay of narrowband components of wideband reflected location signals are predicted for current state with respect to reference, these performances are initial data for OTL location monitoring.

ACKNOWLEDGMENT

The author is grateful to R.G. Minullin, as well as employees of OJSC “Grid Company” of the Republic of Tatarstan for their technical support.The work was performed with financial support from the Ministry of Science and Higher Education of the Russian Federation under Agreement No. 14.574.21.0141 dated September 26, 2017, the unique project identifier RFMEFI57417X041.

REFERENCES

1. R.G. Minullin, V.A. Kasimov, M.R. Yarullin. Multichannel radar control of icing on wires overhead transmission lines. *2016 2nd International Conference on Industrial Engineering, Applications and Manufacturing (ICIEAM)*, 2016, pp. 1-6. IEEE Conference Publications.
2. R.G. Minullin, V.A. Kasimov, T.K. Filimonova, R.M. Gazizullin, A.S. Minkin. Locational Device for Detecting Damages and Ice Deposits on Overhead Power Transmission Lines. *International Journal of Mechanical Engineering and Technology (IJMET), 2017*, Vol. 8(10), pp. 680–687.
3. R.G. Minullin, V.A. Kasimov, T.K. Filimonova, R.M. Gazizullin, A.S. Minkin. Reflectometry Method of Ice Detection on Wires of Overhead Transmission Lines. *International Journal of Mechanical Engineering and Technology (IJMET)*, 2017, Vol. 8(10), pp. 688–698.

4. R. Minullin, I. Fardiev. The use of the location method for detecting damage to transmission lines. *International Journal of Mechanical and Production Engineering Research and Development*, 2018, vol. 9(11), pp. 2057-2069.
5. V.A. Kasimov, R.G. Minullin. Radar Detection of Ice and Rime Deposits on Cables of Overhead Power Transmission Lines. *Power Technology and Engineering*, 2019, Vol. 52(6), pp. 736-745.
6. R.G. Minullin. Connection of diagnostic location equipment to overhead power lines. *Energetic*, 2017, vol. 10, pp. 10–14.
7. V.A. Kasimov, R.G. Minullin. Processing of reflectograms for sensing overhead power lines. *Proceedings of the VII International Scientific and Technical Conference "Electric Power Industry through the Eyes of Youth"*. In 3 V. 3. Kazan: KGEU, 2016, pp. 65-68.
8. O.V. Lazorenko, L.F. Chernogor. Ultra-wideband signals and physical processes. 2. Methods of analysis and application. *Radiophysics and radio astronomy*, 2008, vol. 13(4), pp. 270-322.
9. O.V. Lazorenko, L.F. Chernogor. Ultra-wideband signals and physical processes. 1. Basic concepts, models and methods of description. *Radiophysics and radio astronomy*, 2008, Vol. 13(2), pp. 166-194.
10. Time-Frequency Analysis methods, including the Wigner-Ville Distribution: Applications to Transient Signals. Available: http://case.caltech.edu/tfr/. 25.03.2019.
11. N. E. Huang, S. R. Shen Z .Long., M. C. Wu, H.H. Shih, Q. Zheng, N.-C. Yen, C. C. Tung, H.H. Liu. Spectrum for nonlinear and non-stationary time series analysis. *Proc. R. Soc. Lond. A*, 1998, vol. 454, pp. 903–995.
12. R.R. Nigmatullin, G. Maione, P. Lino, F. Saponaro, W. Zhang. The general theory of the Quasi-reproducible experiments: How to describe the measured data of complex systems? *Communications in Nonlinear Science and Numerical Simulation*, 2017, vol. 42, pp. 324-341.